Atmospheric
Measurement
Techniques
Discussions

1 # Calibration of Hydroxyacetonitrile (HOCH$_2$CN) and Methyl

2 # isocyanate (CH$_3$NCO) Isomers using I$^-$ Chemical Ionization

3 # Mass Spectrometry (CIMS)

4

5 Zachary Finewax[1, 2, a], Aparajeo Chattopadhyay[1,2,b], J. Andrew Neuman[1,2], James M. Roberts[1],

6 James B. Burkholder[1,*]

7

8 [1] Chemical Sciences Laboratory, National Oceanic and Atmospheric Administration (NOAA), Boulder, CO, USA

9 [2] Cooperative Institute for Research in Environmental Sciences (CIRES), University of Colorado, Boulder, CO,

10 USA

11 [a] Present address: Air Pollution Control Division, Colorado Department of Health and Environment, Denver, CO,

12 USA

13 [b] Present address: Department of Earth and Environmental Sciences, University of Rochester, Rochester, NY, USA

14

15 *Correspondence to*: James B. Burkholder (James.B.Burkholder@noaa.gov)

16

17 **Abstract.** The toxic reduced nitrogen compound methyl isocyanate (CH$_3$NCO, MIC) has been

18 reported present in wildfire and bio-mass burning emissions, agricultural fumigation plumes, and

19 indoor air. Its isomer, hydroxyacetonitrile (HOCH$_2$CN, glycolonitrile, HAN) has not been

20 observed in the Earth's atmosphere to date. In this study, absolute sensitivity calibrations for these

21 isomers using two I$^-$ chemical ionization mass spectrometry (I-CIMS) instruments, time-of-flight

22 (ToF) and quadrupole (Quad) instruments, commonly used in laboratory and field measurements,

23 were performed, for the first time, over a range of ion-molecule reactor temperature (10–40°C)

24 and I(H$_2$O)$^-$/I$^-$ ratio (0.01–1). This study demonstrates that I-CIMS, under typical operating

25 conditions, is not sensitive to MIC with limits of detection (LOD) of >860 and >570 ppb for the

26 ToF and Quad I-CIMS instruments, respectively. Both I-CIMS instruments are, however, highly

27 sensitive to the HAN isomer with 0.3 and 3 ppt LODs for the ToF-CIMS and Quad-CIMS

28 instruments, respectively. These results contradict several recent field studies that have reported

29 the detection of MIC using I-CIMS instruments. This study demonstrates that HAN, rather than

30 MIC, was most likely the C$_2$H$_3$NO isomer observed in those field studies, although the source

31 chemistry for HAN remains uncharacterized.

32

Atmospheric
Measurement
Techniques

Discussions

1 Introduction

The identification and quantitative measurement of atmospheric trace species are critical elements in the development of air quality models and the establishment of environmental policies. Methyl isocyanate (CH_3NCO, MIC) and hydroxyacetonitrile ($HOCH_2CN$, glycolonitrile, HAN) (Wolfsie, 1960) are toxic reduced nitrogen isomers present in an extreme range of environments. MIC has been reported in wildfire and bio-mass burning, e.g., Koss et al. (2018), and building fire emissions (Blomqvist et al., 2003), agricultural fumigation plumes (Woodrow et al., 2014), and indoor air (Bekki et al., 2018), particularly where there is cigarette smoke (Moldoveanu, 2010), cooking emissions, and chlorine-disinfectant use. HAN has been observed spectroscopically in interstellar space (see Zhao et al. (2021) and references within), while measurements in the Earth's atmosphere have not been reported to date. The atmospheric degradation of MIC leads to the formation of isocyanic acid (HNCO) (Papanastasiou et al., 2020), another toxic reduced nitrogen compound. The atmospheric chemistry of the HAN isomer is not presently characterized.

The implementation of I⁻ chemical ionization mass spectrometry (I-CIMS) instruments, in particular high-resolution time-of-flight mass spectrometer instruments (I-CIMS ToF-MS), has enabled high sensitivity laboratory and ground-based field measurements as well as high spatial and temporal resolution in airborne field studies. However, a general limitation of CIMS measurements is the inability to distinguish isomers, e.g., MIC and HAN C_2H_3NO isomers, without using pre-separation techniques such as gas chromatography. Field measurements of MIC have been reported in outdoor (Priestley et al., 2018) and indoor (Mattila et al., 2020a; Mattila et al., 2020b; Wang et al., 2022) environments using (I-CIMS) instruments, with sensitivity calibration estimated using voltage-scan techniques (Mattila et al., 2020b; Wang et al., 2022) and analogy to the sensitivity of other VOC species (Priestley et al., 2018).

The primary objective of this work was to establish sample handling and I-CIMS sensitivity calibration protocols for the C_2H_3NO MIC and HAN isomers. Absolute pressure and FTIR measurements were used to establish MIC standards, while diffusion and infusion methods, coupled with total reactive nitrogen (N_r) methods, were used for the quantification of HAN standards. Calibration measurements are presented for I-CIMS time-of-flight (ToF-CIMS) and quadrupole CIMS (Quad-CIMS) mass spectrometry instruments over a range of $I(H_2O)^-/I^-$ ratios and ion-molecule reactor (IMR) temperatures. The results from this work can be applied to similar instruments used in laboratory and field studies, although instrument sensitivities may vary somewhat depending on instrument configuration and operating conditions. This work demonstrates that the recent field measurements reported by Priestley et al. (2018), Mattila et al. (2020a), and Wang et al. (2022) have mis-attributed their measured I-CIMS signal, which was assigned to MIC, when it was most likely due to HAN.

2 Experimental Methods

A primary goal of this work was the development of measurement protocols for hydroxyacetontrile ($HOCH_2CN$, HAN) and methyl isocyanate (CH_3NCO, MIC) using iodide chemical ionization mass spectrometry (I-CIMS) with a time-of-flight mass spectrometer (ToF-CIMS) (Lee et al., 2014) and quadrupole mass spectrometer (Quad-CIMS) (Neuman et al., 2000) instruments. We have focused on calibration measurements for ToF-CIMS and Quad-CIMS instruments for which calibrations for MIC and HAN have not been performed previously. An emphasis in this work was placed on MIC and HAN sample handling and quantification, i.e., knowing what the sample concentration is at the instrument inlet.

71   MIC and HAN samples for calibration measurements were prepared using dilute gas mixtures prepared using

72   absolute pressure measurements, diffusion sources, and infusion sources that are described in detail below. Absolute

73   concentrations were determined using FTIR spectroscopy (MIC) and a total reactive nitrogen (N_r) instrument (HAN).

74   Calibration measurements were performed with ToF- and Quad-CIMS instruments to evaluate differences in

75   sensitivity for instruments with different configurations, e.g., ion-molecule reactor (IMR) geometries, ionization

76   sources, and ion focusing optics. In addition, sensitivities were determined for a range of IMR temperature (10–40°C)

77   and $I(H_2O)^-/I^-$ ratios, commonly used in laboratory and field studies, which are known to affect I-CIMS sensitivity

78   (see Robinson et al. (2022)). The MIC and HAN calibration methods, N_r instrument and methods, and ToF- and

79   Quad-CIMS instruments are described below.

2.1 Methyl isocyanate source and calibration

81   Methyl isocyanate (MIC) is a stable volatile liquid at room temperature with a vapor pressure of ~467 hPa (1 hPa =

82   0.75 Torr) at 25°C. For the present study, a MIC sample was obtained commercially in pure form. Dilute gas-phase

83   methyl isocyanate (MIC) samples were prepared manometrically at a total pressure of 1066 hPa in a 12 L Pyrex bulb

84   with He bath gas. The MIC mixing ratio was ~3.5%. The MIC mixing ratio was also determined by Fourier transform

85   infrared spectroscopy using the absorption cross section data measured in Papanastasiou et al. (2020) from this

86   laboratory. Dilute high-pressure gas standards were prepared by diluting glass bulb standards into aluminum cylinders

87   and filled with zero air. Methyl isocyanate standards were quantitatively added to the calibrated zero air flow sampled

88   by the I-CIMS instruments.

2.2 Hydroxyacetonitrile (HAN) source and calibration methods

90   HAN is a stable semi-volatile compound, vapor pressure of 1.33 hPa at 336 K (NIOSH), that is available commercially

91   as a 70 wt% mixture with H_2O. Over the course of this study, liquid-to-gas-phase diffusion and infusion methods

92   were applied for the delivery of gas-phase HAN to the N_r calibration and I-CIMS instruments.

93   The diffusion source is described in detail elsewhere (Roberts et al., 2010; Williams et al., 2000). Basically, a

94   capillary diffusion cell regulated vapor from the liquid sample into the gas stream feeding into the N_r and I-CIMS

95   instruments. The concentration of source compound is regulated by varying the total gas flow, i.e., dilution factor.

96   This source method requires an independent determination of the compound concentration in the gas stream. The

97   infusion method has been used previously in our laboratory and is described in detail elsewhere (Bernard et al., 2017;

98   Bernard et al., 2018). Basically, a syringe pump is used to deliver a constant liquid flow (0.01–0.3 µL min⁻¹ in our

99   experiments) of a HAN sample into the gas stream feeding into the N_r and I-CIMS instruments. The region of the

100 liquid-gas interface was heated (40 to 60°C) to ensure uniform volatilization and minimize potential sample

101 condensation. Measurements were performed using the commercially available stock HAN solution and a HAN

102 sample diluted in acetone, prepared off-line. The mixing ratio of HAN in the gas flow can in principle be calculated

103 using the calibrated gas and liquid flow rates, the density of the compound, and its liquid mixing ratio, although in

104 this work, the HAN infusion source was calibrated using a total reactive nitrogen, N_r, measurement.

2.3 Total reactive nitrogen, N_r, measurement

106 The infusion source gas-phase concentration of HAN was determined by a total reactive nitrogen, N_r, measurement.

107 Total reactive nitrogen is defined as all reduced and oxidized nitrogen-containing compounds with the exception of

108   N$_2$ and N$_2$O. The N$_r$ instrument has been demonstrated for both gas-phase and particle-phase N$_r$, and is described in

109   detail elsewhere (Stockwell et al., 2018). In this study, the nitrogen containing compounds in a gas-phase sample are

110   first catalytically converted on a 750°C Pt catalyst to NO and NO$_2$. The NO$_2$ is subsequently converted to NO on a

111   molybdenum oxide catalyst at 350°C. The NO then reacts with an excess of O$_3$ to form NO$_2$, which is detected by

112   chemiluminescence (Williams et al., 1998). The N$_r$ instrument was calibrated using commercial dilute mixtures of

113   NO (5.18 ppm) and HCN (9.5 ppm) in a N$_2$ bath gas. HCN and NO calibrations performed over the course of the

114   study agreed to within 3%. The total flow through the N$_r$ instrument was set to 1.048 sLPM (standard liter per minute)

115   and the total zero air flow from the infusion source was 2.148 sLPM. The excess flow passed through an exhaust line.

116   Considering uncertainties in the standards and flow rates, the 2σ uncertainty in the N$_r$ calibration of the HAN source

117   was estimated to be 15%. The HAN infusion source was calibrated by measuring the N$_r$ concentration as a function

118   of the liquid injection flow rate. Over the course of the study, multiple calibration experiments were performed using

119   independently prepared HAN samples.

120   **2.4 Iodide Chemical Ionization Mass Spectrometry (I-CIMS)**

121   I-CIMS has the ability to measure sub-part per trillion (ppt) gas-phase concentrations of organic acids, halogens,

122   oxidized organic compounds, and N$_2$O$_5$ at up to 10 Hz resolution (Huey, 2007; Neuman et al., 2000; Veres et al.,

123   2020). This relatively soft ionization technique usually yields an I$^-$ cluster ion with the intact analyte molecule. I-

124   CIMS is highly selective, with the sensitivity to an analyte dependent on the binding enthalpy of the compound with

125   I$^-$. Time-of-flight mass spectrometers typically contain ion focusing quadrupoles that can also impart changes to the

126   sensitivity of analytes due to mass-dependent ion transmission and collision-induced dissociation (Robinson et al.,

127   2022). The I-CIMS instruments used in the present study have been described in detail previously and only pertinent

128   details are described below.

129   **2.4.1 Time-of-Flight Chemical Ionization Mass Spectrometer (ToF-CIMS)**

130   The ToF-CIMS is setup with a pressure-controlled inlet, ion molecule reactor (IMR), small segmented quadrupole

131   (SSQ), big segmented quadrupole (BSQ), and time-of-flight (ToF) mass analyzer (Veres et al., 2020). A Kr lamp

132   provided vacuum ultraviolet radiation at 124 and 117 nm that photoionized CH$_3$I to produce I$^-$ in the IMR

133   (Breitenlechner et al., 2022; Ji et al., 2020). Analytes (A) react with I$^-$ or I(H$_2$O)$^-$ to form adducts:

134    $I^- + A \leftrightarrow [I\text{-}A]^-$ (1)

135    $[I\text{-}H_2O]^- + A \leftrightarrow [I\text{-}A]^- + H_2O$ (2)
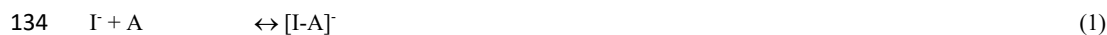
136   with I-C$_2$H$_3$NO$^-$ detected at m/z 183.9265. Key instrument conditions that impact the sensitivity for an analyte are the

137   IMR temperature and I(H$_2$O)$^-$/I$^-$ ratio (Lee et al., 2014; Robinson et al., 2022; Veres et al., 2020). In this study, the

138   IMR was temperature controlled between 20 and 40°C and the I(H$_2$O)$^-$/I$^-$ ratio was dynamically controlled at 0.01,

139   i.e., dry, and over the range 0.4 to 0.6, which represents a typical range of operating conditions of laboratory and field

140   instruments. The ToF-CIMS inlet was pressure controlled at 130 hPa and the flow into the inlet was controlled to 6

141   sLPM. The IMR was pressure controlled to 44 hPa (Zhang and Zhang, 2021). The pressure in the SSQ and BSQ

142   were 1.7 and 0.013 hPa, respectively. The sum of I$^-$ + I(H$_2$O)$^-$ was typically 5MHz in these experiments.

143   **2.4.2 Quadrupole Chemical Ionization Mass Spectrometer (Quad-CIMS)**

144 The Quad-CIMS instrument setup consisted of a critical orifice inlet (600 μm dia.) combined with an IMR, ion

145 focusing lenses, and a quadrupole mass analyzer (Neuman et al., 2000). I^- ions were generated by passing a 0.1%

146 CH_3I in N_2 mixture through a ^{210}Po radioactive source. The IMR was temperature controlled between 10 and 30°C.

147 The $I(H_2O)^-/I^-$ ratio was adjusted between 0.01–1.0 by controlling the humidity of the gas flow into the CIMS, which

148 ranged from 4.2 to 4.5 sLPM. This system did not have an intermediate pressure zone between the IMR and mass

149 spectrometer chamber, common to many I-CIMS instruments, that would serve as a collisional-dissociation chamber.

150 The pressure in the IMR was maintained at 37 hPa by varying the pumping speed. The mass resolution of the Quad-

151 CIMS instrument is ~200 and that of the ToF-CIMS is ~5000. The sum of I^- + $I(H_2O)^-$ was typically 500 kHz in these

152 experiments.

153 **2.5 Materials**

154 Synthetic air (zero grade), N_2 (UHP, 99.999%), He (UHP, 99.999%) gases and CH_3I (99%) and acetone (99%) were

155 used as provided. Standard dilute mixtures of NO (5.18 ppm in N_2) and HCN (9.5 ppm in N_2) were obtained

156 commercially. Hydroxyacetonitrile (HAN, ~70% in H_2O, CAS RN: 107-16-4) and methyl isocyanate (MIC, 97+%,

157 CAS RN: 624-83-9) samples were obtained commercially. The MIC sample contained a <3% trimethylchlorosilane

158 (CAS RN: 75-77-4) inhibitor. The HAN and MIC samples were degassed in freeze—pump—thaw cycles. Samples

159 were stored in a chemical refrigerator in vacuum sealed Pyrex reservoirs prior to use.

160 A dilute (3.48%) gas mixture of MIC in He was prepared manometrically in a 12 L Pyrex bulb. Fourier transform

161 infrared spectroscopy (FTIR) measurements (1 cm^{-1} resolution, 425 cm pathlength) using a previously determined

162 absorption spectrum from our laboratory (Papanastasiou et al., 2020) confirmed the mixing ratio, to within 10% of the

163 manometric preparation. Standard dilute solutions of HAN in acetone were prepared volumetrically using 1.0–2.0 μL

164 of the commercial HAN solution and 5.0 or 10.0 mL of acetone. The standard solutions were stored in a chemical

165 refrigerator in vacuum sealed Pyrex reservoirs. Samples used in the calibration infusion experiments were extracted

166 from the standard solution with a gas-tight 10 or 100 μL syringe.

167 **3. Results and Discussion**

168 **3.1 Methyl isocyanate (CH_3NCO, MIC)**

169 ToF-CIMS and Q-CIMS measurements with MIC mixing ratios of up to 860 ppb yielded no measurable signal for the

170 I-MIC^- or $I(H_2O)$-MIC^- adducts above the background (1σ background noise level of 3 ncps). Measurements were

171 performed over the range of CIMS conditions described in the experimental section. The sensitivity upper-limits

172 obtained are given in **Table 1**, and represent the signal increase (normalized to 1 million cps of the sum of I^- + $I(H_2O)^-$

173 per mixing ratio unit increase of the compound). Our measurements indicate that MIC mixing ratios of greater than

174 1 ppm may be required to generate a detectable I-CIMS signal, if MIC can be detected by I-CIMS at all.

175 **Table 1.** ToF-CIMS and Quad-CIMS instrument sensitivity (S) and limits of detection (LOD) measured in this work
176 for hydroxyacetonitrile ($HOCH_2CN$, HAN) and methyl isocyanate (CH_3NCO, MIC) for typical field operating
177 conditions with an IMR temperature of 30°C, $I(H_2O)^-/I^-$ ratio of 0.55, and 1 s integration. See **Fig. 3** for sensitivity
178 dependence on operating conditions.

	CH_3NCO (MIC)		$HOCH_2CN$ (HAN)	
Instrument	S	LOD	S	LOD

|	(ncps ppb^{-1})	(ppb)	(ncps ppt^{-1})	(ppt)
ToF-CIMS	<0.009	>860	19.6 ± 0.5	0.3
Quad-CIMS	<0.044	>570	25.8 ± 0.7	3

179   The ToF- and Quad-CIMS instruments used in the present study were found to be insensitive to the detection of
180   CH_3NCO (MIC). The lack of MIC sensitivity for both instruments suggests that the I$^-$ cluster with MIC is not
181   thermodynamically stable in the IMR. The ion focusing or ion optics in the ToF-CIMS and the Quad-CIMS are,
182   however, quite different. The ToF-CIMS SSQ was set to 1.7 hPa, so collisions occur in this region, resulting in some
183   collisional dissociation. The BSQ focuses ions and can also result in fragmentation of I$^-$ clusters. The ion optics of
184   the Quad-CIMS uses only static electric fields in a low-pressure region (<1.3×10^{-4} hPa) and does not have sufficient
185   frequency to dissociate I$^-$ clusters. Given the lack of sensitivity of both ToF- and Quad-CIMS instruments to MIC, it
186   is unlikely that other common I-CIMS instrument configurations have the sensitivity to detect MIC at atmospherically
187   relevant mixing ratios.

188   **3.2 Hydroxyacetonitrile (HOCH$_2$CN, HAN)**

189   The diffusion source, with the commercial 70% HAN/H$_2$O solution, proved to be an unsuccessful HAN delivery
190   method. This method produced high gas-phase concentrations of an HCN impurity as identified by I-CIMS. Although
191   HCN was a minor sample impurity, <1%, its high vapor pressure (862 hPa at 295 K (Perry and Porter, 1926)) and low
192   Henry's law coefficient (~9 M Atm^{-1} (Burkholder et al., 2019)), resulted in a [HCN]/[HAN] gas-phase mixing ratio
193   of greater than 1000, i.e., HAN was not detectable by I-CIMS using this source. The high gas-phase HCN
194   concentration, using the diffusion method, precluded quantitative calibration of HAN concentration using the total
195   reactive nitrogen calibration method.
196   The infusion source did not produce detectable gas-phase HCN above the detection limit of the mass spectrometers,
197   i.e., the HCN impurity level was much less than 1%. Therefore, HCN did not influence the absolute HAN calibration
198   determination using the N$_r$ instrument. The region around the infusion source was heated to 50°C when using the
199   commercially available HAN stock solution. Although this source worked, it didn't provide a stable HAN signal to
200   within 10%. This source, using a dilute HAN/acetone mixture with the region of the infusion source heated to 45°C,
201   i.e., slightly below the boiling point of acetone, yielded more stable HAN signals with variations of a few percent.
202   Measurements performed at temperatures greater than 45°C yielded reasonable results, but the signal was less stable
203   due most likely to boiling of the acetone solvent.
204   Calibration of hydroxyacetonitrile (HAN) solutions by total reactive nitrogen (N$_r$) is shown in **Fig. 1**. The infusion
205   method produces a stable source of HAN with a high signal-to-noise ratio for a typical calibration experiment. The
206   total HAN concentration was set by adjusting the injection flow rate. Individual solutions were calibrated multiple
207   times, as shown in **Fig. 1**. The 2σ uncertainty of the fit precision of [HAN] vs. infusion flow rate was determined to
208   be 4%. The small positive intercept may be due to minor unidentified N$_r$ impurities.
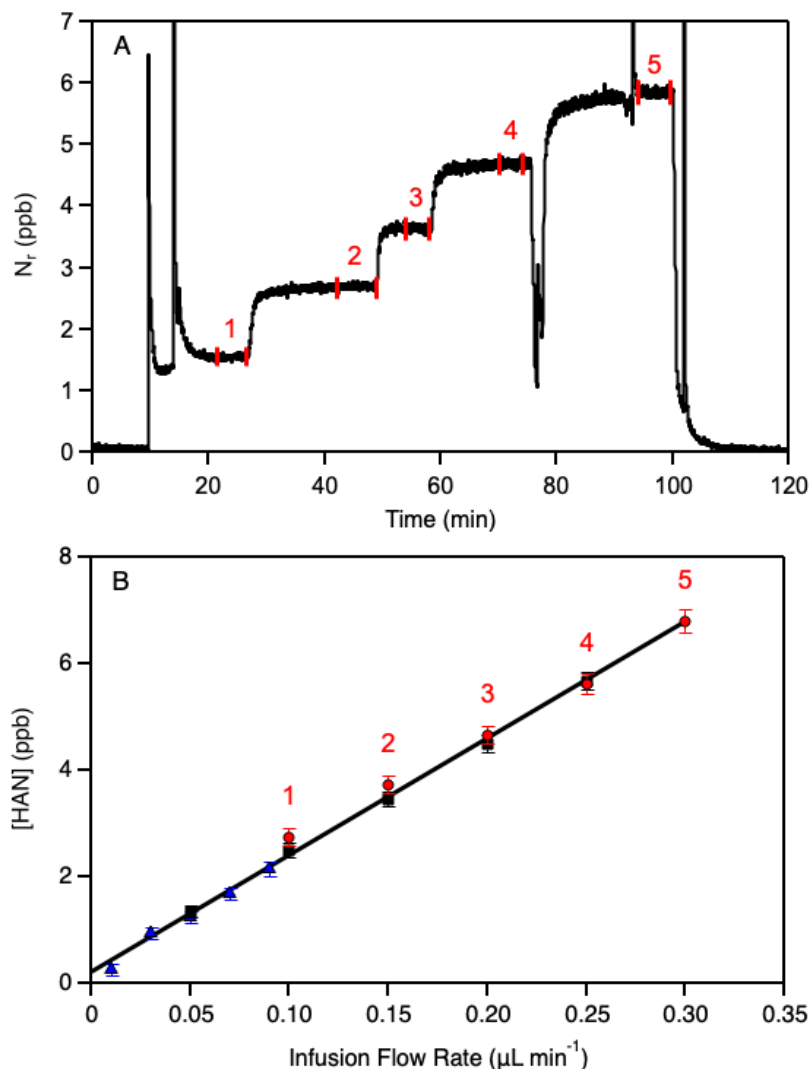
Figure 1: Calibration of the hydroxyacetonitrile (HOCH$_2$CN, HAN) infusion source at 23°C using the total nitrogen, N$_r$, instrument (see text for details of the N$_r$ instrument). **(a)** Background-corrected time series of a representative calibration experiment. The data within the numbered vertical lines were averaged and correspond to the numbered points in panel b. **(b)** Calibration of HAN concentration as a function of infusion source flow rate. Different symbols represent independent calibration experiments. The line is an unweighted linear least-squares fit of all the data. Error bars represent 2σ measurement precision.

Calibrations of the HAN signal on the ToF-CIMS and Quad-CIMS instruments were made by varying the infusion flow rate, see representative data for the Quad-CIMS in **Fig. 2**. The obtained ToF- and Quad-CIMS sensitivity for HAN given in **Table 1** was obtained using the infusion method with the dilute HAN/acetone samples. For typical field operating conditions with an IMR temperature of 30°C, I(H$_2$O)$^-$/I$^-$ ratio of 0.55, and 1 s integration the HAN sensitivity of the ToF I-CIMS was determined to be ~20 ncps ppt^{-1}.

Atmospheric
Measurement
Techniques
Open Access
Discussions
EGU
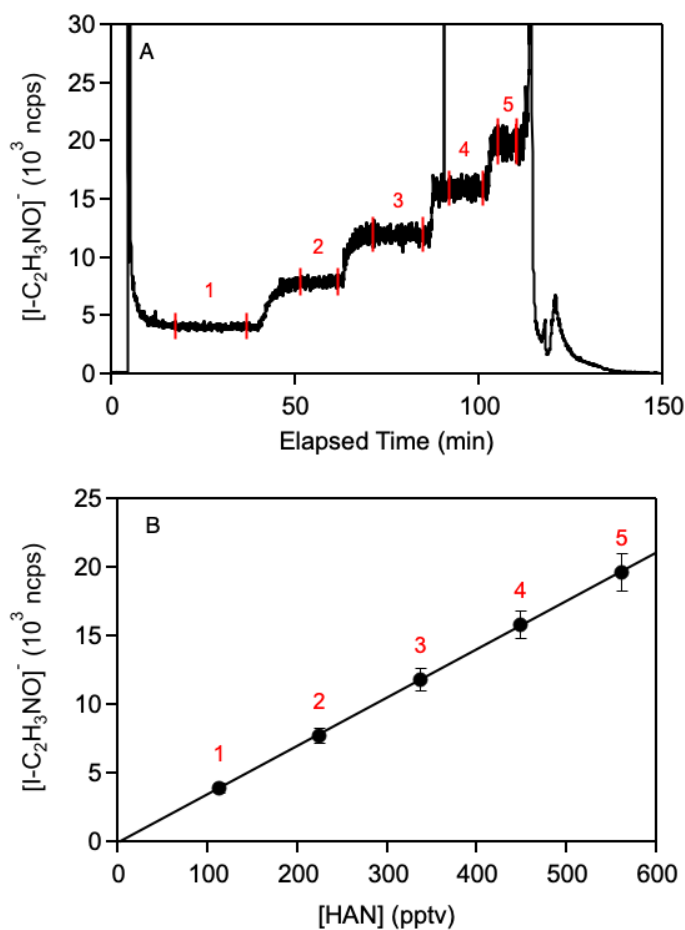
Figure 2: Calibration of the Quad-CIMS instrument using the hydroxyacetonitrile (HOCH$_2$CN, HAN) infusion source at 23°C (see text for details of the Quad-CIMS instrument). (a) Background-corrected time series of a representative Quad-CIMS calibration experiment (IMR temperature = 20°C, I(H$_2$O)$^-$/I$^-$ = 0.57). The data within the numbered vertical lines were averaged and correspond to the numbered points in panel B. (b) Quad-CIMS HAN calibration curve where the HAN concentration was determined from the N$_r$ calibration of the infusion source, e.g., see **Fig. 1**. The line is an unweighted linear least-squares fit of the data. Error bars represent 2σ measurement precision.

The HAN concentration from the infusion source at the instrument inlet was varied, for each IMR temperature and I(H$_2$O)$^-$/I$^-$ ratio, to determine the HAN sensitivity temperature and I(H$_2$O)$^-$/I$^-$ dependence shown in **Fig. 3**. The ToF-CIMS and Quad-CIMS instruments are both highly sensitive to HAN, but displayed slightly different temperature and I(H$_2$O)$^-$/I$^-$ dependencies. As the temperature increased, the HAN sensitivity decreased consistent with the [I-HAN]$^-$ adduct being less stable at higher temperatures. For the ToF-CIMS instrument, the HAN sensitivity decreased a factor of ~1.5–2 between 20 and 40°C at the highest I(H$_2$O)$^-$/I$^-$ ratio included in this study. For the Quad-CIMS instrument, a ~25% decrease in HAN sensitivity was observed at a I(H$_2$O)$^-$/I$^-$ ratio of 1 when increasing the IMR temperature from 10 to 30°C. The I(H$_2$O)$^-$/I$^-$ dependency for HAN sensitivity was fit reasonably well with a quadratic dependence on I(H$_2$O)$^-$/I$^-$: A + B(I(H$_2$O)$^-$/I$^-$) – C(I(H$_2$O)$^-$/I$^-$)^2, where the constant term represents HAN clustering with I$^-$, reaction 1; the linear term represents HAN undergoing a ligand switching reaction with I(H$_2$O)$^-$, reaction 2; and the quadratic term may represent a lack of reactivity of higher-order H$_2$O clusters, I(H$_2$O)$_n^-$ where n >1 or a shift in the

238     $(I\text{-}HAN)^- + H_2O \leftrightarrow (I\text{-}H_2O)^- + HAN$ (3)

239   equilibrium.

240
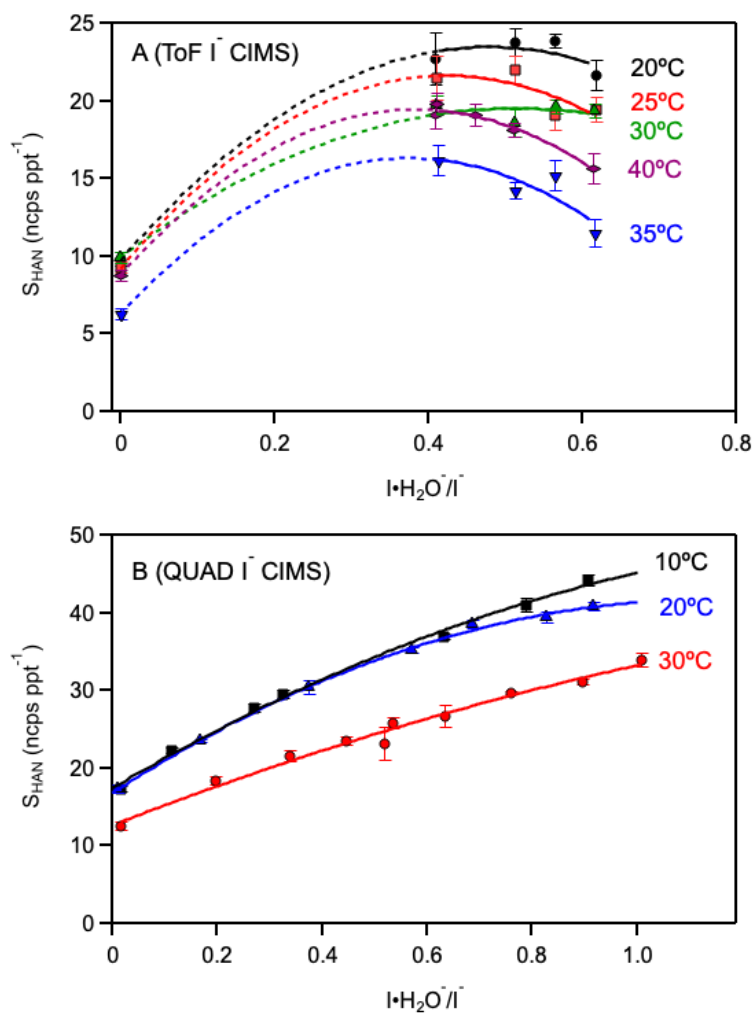
Figure 3: Hydroxyacetonitrile (HOCH$_2$CN, HAN) calibration factors for the ToF and QUAD mass spectrometers used in this work as a function of the $I(H_2O)^-/I^-$ ratio and ion-molecule reactor, IMR, temperature. Error bars represent 2σ precision of the linear calibration fits. Lines are empirical polynomial fits to guide the eye. (a) HAN calibration factors measured for the ToF-CIMS. Symbols represent IMR temperatures of 20°C (black circles), 25°C (red squares), 30°C (green triangles), 35°C (blue upside-down triangles), and 40°C (purple diamonds). (b) Quad-CIMS HAN calibration data. Symbols represent IMR temperatures of: 10°C (black squares), 20°C (blue triangles), 30°C (red circles).

247   There is a plausible explanation for the differences in the Quad-CIMS and ToF-CIMS instrument $I(H_2O)^-/I^-$

248   sensitivity dependence. First, there are differences in these instruments in the ion focusing downstream of the IMR.

249   The ToF-CIMS contains an SSQ at 1.73 hPa that imparts an electric field and acts as a collisional dissociation chamber.

250   The subsequent BSQ also imparts an electric field that can dissociate weakly bound I^- clusters. The $I(H_2O)^-/I^-$ is

251   dynamically controlled in the ToF-CIMS by what is observed at the detector. Therefore, the $I(H_2O)^-$ (and $I(H_2O)_n^-$)

252   ion counts are not representative of the $I(H_2O)^-/I^-$ ratio in the IMR, i.e., the $I(H_2O)^-/I^-$ ratio in the IMR is being under-

253   estimated, although we were unable to quantify the dependence. The Quad-CIMS, which has ion lenses at low-

254   pressure downstream of the IMR, $1.3–0.13) \times 10^{-3}$ hPa, should have only minor collisional dissociation, if any.

255   Therefore, the $I(H_2O)^-/I^-$ ratio measured by the Quad-CIMS is, most likely, close to the actual $I(H_2O)^-/I^-$ in the IMR.

256   In conclusion, it is recommended that instruments used to quantify HAN be calibrated under actual operating

257   conditions. The protocols presented in this work can be used for the calibration of HAN.

258   **4 Conclusions**

259   In this study, protocols for determining I-CIMS instrument sensitivity for CH_3NCO (MIC) and $HOCH_2CN$ (HAN),

260   two stable toxic C_2H_3NO isomers (Panda et al., 2023), were developed. Calibration of ToF-CIMS and Quad-CIMS

261   instruments for HAN were performed over a range of instrument conditions commonly used in laboratory and field

262   experiments, including: ion molecule reactor (IMR) temperature (10–40°C) and $I(H_2O)^-/I^-$ ratios between 0.1 and 1.

263   Both I-CIMS instruments were found to be highly sensitive to HAN with 0.3 and 3 ppt limits of detection (LOD) for

264   the ToF-CIMS and Quad-CIMS instruments, respectively, for measurements with the IMR at 30°C, $I(H_2O)^-/I^-$ ratio of

265   0.55, and 1 s integration (see **Table 1**). The instruments were insensitive to MIC with LODs of >860 and >570 ppb

266   for the ToF and Quad I-CIMS instruments, respectively. A weak negative temperature dependence and systematic

267   positive $I(H_2O)^-/I^-$ ratio dependence was observed for HAN. The ToF and Quad I-CIMS instruments have similar

268   normalized sensitivities, reflecting the similar chemistry in the ion molecule reaction regions. The ToF instrument

269   has much lower LOD because the reagent ion concentration was approximately 10 times greater than that in the Quad

270   instrument and the ToF has far better mass resolution. The results from this study should, to a first approximation,

271   translate to other laboratory and field I-CIMS instruments.

272   Our work demonstrates that the previous field studies of Priestley et al. (2018), Mattila et al. (2020a; 2020b), and

273   Wang et al. (2022), which used I-CIMS detection methods, mis-attributed the C_2H_3NO mass signal as methyl

274   isocyanate, MIC, and also provides evidence for the observation of HAN, a previously unrecognized species in these

275   environments. Our results suggest that HAN was observed, but do not imply that MIC was not present in the

276   environments studied by Priestley et al., Mattila et al., and Wang et al. Since I-CIMS is not sensitive to MIC,

277   alternative measurement methods, such as proton transfer CIMS, would be required to identify the presence of MIC.

278   Our work indicates that HAN is commonly present in the troposphere. The heterogeneous and gas-phase atmospheric

279   chemistry of $HOCH_2CN$ (HAN) are, however, not presently characterized. Here, we postulate that in addition to

280   primary HAN emissions, e.g., from wildfires, that HAN would be formed heterogeneously in clouds, or on hydrated

281   aerosol, via the liquid-phase reaction:

282    $HCN + H_2CO \Leftrightarrow HOCH_2CN$ (4)

283   The partitioning of HAN between the liquid- and gas-phase will depend on its Henry's law coefficient, which has not

284   been measured to date. Sander (2023) reports an estimated Henry's law coefficient value of ~130 M atm^{-1}, using a

285   quantitative structure-property relationship, which implies partitioning of HAN into the gas-phase. HCN and H_2CO

Atmospheric
Measurement
Techniques
Discussions
Open Access
EGU

286 are ubiquitous in the atmosphere with elevated concentrations in wildfire plumes, which may lead to a significant
287 enhancement of the HAN concentration following a wildfire plume exposure to clouds. Our work will aid future
288 laboratory and field studies to identify the atmospheric source chemistry of HAN as well as its atmospheric loss
289 processes and degradation products.

290 *Data availability*. NA

291 *Author contributions*. ZF undertook the experimental measurements and contributed to the first draft and writing of
292 the paper. AC performed the MIC infrared measurements and initial ToF MIC measurements. JAN performed the
293 initial ToF MIC measurements. JMR performed the initial Nr measurements and contributed to the writing of the
294 paper. JBB supervised the project and completed the writing of the paper.

295 *Competing interests*. The authors declare that they have no conflict of interest.

298 Review statement.

299

References

300 **References**

301 Bekki, K., Uchiyama, S., and Kunugita, N.: Analysis of isocyanates in indoor dust, Anal. Bioanal. Chem., 410,
302   4247-4251, https://doi.org/10.1007/s00216-018-1110-y, 2018.

303 Bernard, F., Papanastasiou, D. K., Papadimitriou, V. C., and Burkholder, J. B.: Infrared absorption spectra of linear
304   (L2-L5) and cyclic (D3-D6) permethylsiloxanes, J. Quant. Spectros. Rad. Trans., 202, 247-254,
305   https://doi.org/10.1016/j.jqsrt.2017.08.006, 2017.

306 Bernard, F., Papanastasiou, D. K., Papadimitriou, V. C., and Burkholder, J. B.: Infrared absorption spectra of
307    $N(C_xF_{2x+1})_3$, x = 2-5 perfluoroamines, J. Quant. Spectrosc. Rad. Trans., 211, 166-171,
308   https://doi.org/doi:10.1016/j.jqsrt.2018.02.039, 2018.

309 Blomqvist, P., Hertzberg, T., Dalene, M., and Skarping, G.: Isocyanates, aminoisocyanates and amines from fires - a
310   screening of common materials found in buildings, Fire Mater., 27, 275-294,
311   https://doi.org/doi:10.1002/fam.836, 2003.

312 Breitenlechner, M., Novak, G. A., Neuman, J. A., Rollins, A. W., and Veres, P. R.: A versatile vacuum ultraviolet
313   ion source for reduced pressure bipolar chemical ionization mass spectrometry, Atmos. Meas. Tech., 15, 1159-
314   1169, https://doi.org/doi:10.5194/amt-15-1159-2022, 2022.

315 Burkholder, J. B., Sander, S. P., Abbatt, J., Barker, J. R., Cappa, C., Crounse, J. D., Dibble, T. S., Huie, R. E., Kolb,
316   C. E., Kurylo, M. J., Orkin, V. L., Percival, C. J., Wilmouth, D. M., and Wine, P. H.: "Chemical Kinetics and
317   Photochemical Data for Use in Atmospheric Studies, Evaluation No. 19," JPL Publication 19-5, Jet Propulsion
318   Laboratory, Pasadena, 2020 http://jpldataeval.jpl.nasa.gov., 2019.

319 Huey, L. G.: Measurement of trace atmospheric species by chemical ionization mass spectrometry: speciation of
320   reactive nitrogen and future directions, Mass Spectrom. Rev., 26, 166-184,
321   https://doi.org/doi:10.1002/mas.20118, 2007.

322 Ji, Y., Huey, G., Tanner, D. J., Lee, Y. R., Veres, P. R., Neuman, J. A., Wang, Y. H., and Wang, X. M.: A vacuum
323   ultraviolet ion source (VUV-IS) for iodide-chemical ionization mass spectrometry: a substitute for radioactive
324   ion sources, Atmos. Meas. Tech., 13, 3683-3696, https://doi.org/doi:10.5194/amt-13-3683-2020, 2020.

325 Koss, A. R., Sekimoto, K., Gilman, J. B., Selimovic, V., Coggon, M. M., Zarzana, K. J., Yuan, B., Lerner, B. M.,
326   Brown, S. S., Jimenez, J. L., Krechmer, J., Roberts, J. M., Warneke, C., Yokelson, R. J., and de Gouw, J.: Non-
327   methane organic gas emissions from biomass burning: identification, quantification, and emission factors from
328   PTR-ToF during the FIREX 2016 laboratory experiment, Atmos. Chem. Phys., 18, 3299-3319,
329   https://doi.org/10.5194/acp-18-3299-2018, 2018.

330 Lee, B. H., Lopez-Hilfiker, F. D., Mohr, C., Kurten, T., Worsnop, D. R., and Thornton, J. A.: An iodide-adduct
331   high-resolution time-of-flight chemical-ionization mass spectrometer: Application to atmospheric inorganic and
332   organic compounds, Environ. Sci. Technol., 48, 6309-6317, https://doi.org/doi:10.1021/es500362a, 2014.

333 Mattila, J. M., Arata, C., Wang, C., Katz, E. F., Abeleira, A., Zhou, Y., Zhou, S., Goldstein, A. H., Abbatt, J. P. D.,
334   DeCarlo, P. F., and Farmer, D. K.: Dark chemistry during bleach cleaning enhances oxidation of organics and
335   secondary organic aerosol production indoors, Environ. Sci. Tech. Lett., 7, 795-801,
336   https://doi.org/10.1021/acs.estlett.0c00573, 2020a.

337 Mattila, J. M., Lakey, P. S. J., Shiraiwa, M., Wang, C., Abbatt, J. P. D., Arata, C., Goldstein, A. H., Ampollini, L.,
338   Katz, E. F., DeCarlo, P. F., Zhou, S., Kahan, T. F., Cardoso-Saldaña, F. J., Ruiz, L. H., Abeleira, A., Boedicker,
339   E. K., Vance, M. E., and Farmer, D. K.: Multiphase chemistry controls inorganic chlorinated and nitrogenated
340   compounds in indoor air during bleach cleaning, Environ. Sci. Tech., 54, 1730-1739,
341   https://doi.org/10.1021/acs.est.9b05767, 2020b.

342 Moldoveanu, S. C.: Analysis of acrylonitrile and α-methacrylonitrile in vapor phase of mainstream cigarette smoke
343   using a charcoal trap for collection, Contrib. Tobac. Res., 24, https://doi.org/10.2478/cttr-2013-0892, 2010.

344 Neuman, J. A., Gao, R. S., Schein, M. E., Ciciora, S. J., Holecek, J. C., Thompson, T. L., Winkler, R. H.,
345   McLaughlin, R. J., Northway, M. J., Richard, E. C., and Fahey, D. W.: A fast-response chemical ionization mass
346   spectrometer for in situ measurements of HNO_3 in the upper troposphere and lower stratosphere, Rev. Sci.
347   Instrum., 71, 3886-3894, https://doi.org/doi:10.1063/1.1289679, 2000.

348 NIOSH. Glycolonitrile National Institute Occupational Safety Health.

349 Panda, S., Chiranjibi, A., Awasthi, D., Ghoshal, S., and Anoop, A.: Exploring the chemical space of C_2H_3NO
350   isomers and bimolecular reactions with hydrogen cyanide and formaldehyde: Insights into the emergence of life,
351   Earth Space Chem., 7, 1739-1752, https://doi.org/10.1021/acsearthspacechem.3c00113, 2023.

352 Papanastasiou, D. K., Bernard, F., and Burkholder, J. B.: Atmospheric fate of methyl isocyanate, CH_3NCO: OH and
353   Cl reaction kinetics and identification of formyl isocyanate, HC(O)NCO, Earth Space Chem., 4, 1626-1637,
354   https://doi.org/10.1021/acsearthspacechem.0c00157, 2020.

355 Perry, J. H., and Porter, F.: The vapor pressures of solid and liquid hydrogen cyanide, J. Amer. Chem. Soc., 48, 297-
356   300, 1926.

357 Priestley, M., Le Breton, M., Bannan, T. J., Leather, K. E., Bacak, A., Reyes-Villegas, E., De Vocht, F., Shallcross,
358   B. M. A., Brazier, T., Khan, M. A., Allan, J., Shallcross, D. E., Coe, H., and Percival, C. J.: Observations of

359   isocyanate, amide, nitrate, and nitro compounds from an anthropogenic biomass burning using a Tof-CIMS, J.
360   Geophys. Res., 123, 7687-7704, https://doi.org/10.1002/2017jd027316, 2018.
361 Roberts, J. M., Veres, P., Warneke, C., Neuman, J. A., Washenfelder, R. A., Brown, S. S., Baasandorj, M.,
362   Burkholder, J. B., Burling, I. R., Johnson, T. J., Yokelson, R. J., and de Gouw, J.: Measurement of HONO,
363   HNCO, and other inorganic acids by negative-ion proton-transfer chemical-ionization mass spectrometry (NI-
364   PT-CIMS): application to biomass burning emissions, Atmospheric Measurement Techniques, 3, 981-990,
365   https://doi.org/10.5194/amt-3-981-2010, 2010.
366 Robinson, M. A., Neuman, J. A., Huey, L. G., Roberts, J. M., Brown, S. S., and Veres, P. R.: Temperature-
367   dependent sensitivity of iodide chemical ionization mass spectrometers, Atmos. Meas. Tech., 15, 4295-4305,
368   https://doi.org/10.5194/amt-15-4295-2022, 2022.
369 Sander, R.: Compilation of Henry's law constants (version 5.0.0) for water as solvent, Atmos. Chem. Phys., 23,
370   10901-12440, https://doi.org/doi:10.5194/acp-23-10901-2023, 2023.
371 Stockwell, C. E., Kupc, A., Witkowski, B., Talukdar, R. K., Liu, Y., Selimovic, V., Zarzana, K. J., Sekimoto, K.,
372   Warneke, C., Washenfelder, R. A., Yokelson, R. J., Middlebrook, A. M., and Roberts, J. M.: Characterization of
373   a catalyst-based conversion technique to measure total particulate nitrogen and organic carbon and comparison to
374   a particle mass measurement instrument, Atmos. Meas. Tech., 11, 2749-2768, https://doi.org/10.5194/amt-11-
375   2749-2018, 2018.
376 Veres, P. R., Neuman, J. A., Bertram, T. H., Assaf, E., Wolfe, G. M., Williamson, C. J., Weinzierl, B., Tilmes, S.,
377   Thompson, C. R., Thames, A. B., Schroder, J. C., Saiz-Lopez, A., Rollins, A. W., Roberts, J. M., Price, D.,
378   Peischl, J., Nault, B. A., Moller, K. H., Miller, D. O., Meinardi, S., Li, Q. Y., Lamarque, J. F., Kupc, A.,
379   Kjaergaard, H. G., Kinnison, D., Jimenez, J. L., Jernigan, C. M., Hornbrook, R. S., Hills, A., Dollner, M., Day,
380   D. A., Cuevas, C. A., Campuzano-Jost, P., Burkholder, J., Bui, T. P., Brune, W. H., Brown, S. S., Brock, C. A.,
381   Bourgeois, I., Blake, D. R., Apel, E. C., and Ryerson, T. B.: Global airborne sampling reveals a previously
382   unobserved dimethyl sulfide oxidation mechanism in the marine atmosphere, Proc. Nat. Acad. Sci., 117, 4505-
383   4510, https://doi.org/10.1073/pnas.1919344117, 2020.
384 Wang, C., Mattila, J. M., Farmer, D. K., Arata, C., Goldstein, A. H., and Abbatt, J. P. D.: Behavior of isocyanic acid
385   and other nitrogen-containing volatile organic compounds in the indoor environment, Environ. Sci. Tech., 56,
386   7598-7607, https://doi.org/10.1021/acs.est.1c08182, 2022.
387 Williams, E. J., Baumann, K., Roberts, J. M., Bertman, S. B., Norton, R. B., Fehsenfeld, F. C., Springston, S. R.,
388   Nunnermacker, L. J., Newman, L., Olszyna, K., Meagher, J., Hartsell, B., Edgerton, E., Pearson, J. R., and
389   Rodgers, M. O.: Intercomparison of ground-based NO_y measurement techniques, J. Geophys. Res., 103, 22261-
390   22280, doi: 22210.21029/22298JD00074, 1998.
391 Williams, J., Roberts, J. M., Bertman, S. B., Stroud, C. A., Fehsenfeld, F. C., Baumann, K., Buhr, M. P., Knapp, K.,
392   Murphy, P. C., Nowick, M., and Williams, E. J.: A method for the airborne measurement of PAN, PPN, and
393   MPAN, J. Geophys. Res., 105, 28943-28960, https://doi.org/Doi 10.1029/2000jd900373, 2000.
394 Wolfsie, J. H.: Glycolonitrile toxicity, J. Occup. Med., 2, 588-590, 1960.
395 Woodrow, J. E., LePage, J. T., Miller, G. C., and Hebert, V. R.: Determination of methyl isocyanate in outdoor
396   residential air near metam-sodium soil fumigations, J. Agr. Food Chem., 62, 8921-8927,
397   https://doi.org/10.1021/jf501696a, 2014.
398 Zhang, W., and Zhang, H. F.: Secondary ion chemistry mediated by ozone and acidic organic molecules in iodide-
399   adduct chemical ionization mass spectrometry, Anal. Chem., 93, 8595-8602,
400   https://doi.org/10.1021/acs.analchem.1c01486, 2021.
401 Zhao, G., Quan, D., Zhang, X., Feng, G., Zhou, J., Li, D., Meng, Q., Chang, Q., Yang, X., He, M., and Ma, M.-S.:
402   Glycolonitrile ($HOCH_2CN$) chemistry in star-forming regions, Astrophys. J. Supp. Series, 257, 26,
403   https://doi.org/doi:10.3847/1538-4365/ac17ee, 2021.

404

405